1993

Creep Behavior of an Al-2.0 Wt Pct Li Alloy in the Temperature Range 300 °C to 500 °C

Ellison, K.H.; McNelley, T.R.; Fox, A.G.

Ellison, K. H., T. R. McNelley, and A. G. Fox. "Creep behavior of an Al-2. 0 wt pct Li alloy in the temperature range 300° C to 500° C." Metallurgical Transactions A 24.9 (1993): 1993-2001.

http://hdl.handle.net/10945/62120

Creep Behavior of an Al-2.0 Wt Pct Li Alloy in the Temperature Range 300 °C to 500 °C

K.H. ELLISON, T.R. MCNELLEY, and A.G. FOX

The elevated temperature deformation behavior of an Al-2.0 wt pct Li alloy in the temperature range 300 °C to 500 °C was studied using constant extension-rate tension testing and constant true-stress creep testing under both isothermal and temperature cycling conditions. Optical microscopy and transmission electron microscopy (TEM) were employed to assess the effect of deformation on microstructure. The data showed that the stress exponent, n, has a value of about 5.0 at temperatures above the $\alpha + \delta$AlLi solvus (approximately 380 °C) and that subgrains form during plastic deformation. Models for dislocation-climb and dislocation-glide control of creep were analyzed for alloys deformed in the temperature range of stability of the terminal AlLi solid solution. A climb model was shown to describe closely the behavior of this material. Anomalous temperature dependence of the activation energy was observed in this same temperature range. This anomalous behavior was ascribed to unusual temperature dependence of either the Young's modulus or the stacking fault energy, which may be associated, in turn, with a disorder-order transformation on cooling of the alloy.

I. INTRODUCTION

THE addition of Li to Al significantly increases the ambient temperature-elastic modulus while simultaneously reducing the density.[1] As a result, Li-containing Al alloys have attracted great interest from the aerospace industry. Currently, such alloys are intended for use at ambient or lower temperatures, and limitations on maximum use temperatures due to creep have not been determined for engineering Al-Li alloys. Studies by Park *et al.*[2,3] have considered the deformation of Al-2.1 wt pct Li at temperatures of 500 °C and above and have shown that creep of this alloy is controlled by dislocation climb in the same manner as creep of pure Al in this temperature range. Park *et al.*[2] also proposed that this alloy would exhibit a transition from dislocation-climb to dislocation-glide control of creep as the deformation temperature is reduced. Data were not available for temperatures between the $\alpha + \delta$AlLi solvus and 500 °C; thus, this proposal could not be assessed. Measurements of the stress and temperature dependence of creep are necessary to interpret the effect of Li on the creep of Al.

Lithium exhibits significant solid solubility in Al,[4] and so Al-Li alloys may be considered as ordinary solid solutions in the elevated temperature regime. The creep response of Al-X binary solid solutions has been described in one of two ways: (1) those alloys in which dislocation climb is the rate-controlling step during deformation; and (2) where dislocation glide becomes rate controlling due to solute drag on moving dislocations.[5,6,7] Creep of climb-controlled alloys at elevated temperatures is often evaluated using the phenomenological relation

$$\dot{\varepsilon}_c = K_1 \frac{D_{\text{eff}}}{\mathbf{b}^2} \left(\frac{\sigma}{E}\right)^5 \qquad [1]$$

where $\dot{\varepsilon}_c$ is the creep rate, K_1 is a constant, D_{eff} is the effective diffusion coefficient, $\mathbf{b}$ is the Burgers vector, σ is the stress, and E is the Young's modulus.[5,8,9] For glide-controlled alloys, an equation of the form

$$\dot{\varepsilon}_g = K_2 \frac{D_{\text{sol}}}{A} \left(\frac{\sigma}{E}\right)^3 \qquad [2]$$

may be used, where K_2 is a constant, D_{sol} is the solute diffusion coefficient, and A is a constant describing the interaction between dislocations and the diffusing solute atoms.[5,6,7,10,11,12]

For experimental data, the stress exponent, n, is given by

$$n = \left[\frac{\partial \log \dot{\varepsilon}}{\partial \log \sigma}\right]_T \qquad [3]$$

and may be determined from double logarithmic plots of strain rate *vs* stress. If $n = 5$, then it is inferred that dislocation climb is likely to be rate controlling. In these circumstances, well-defined subgrain structures are observed to form during creep.[5–8] If $n = 3$, then it is surmised that dislocation glide controls plastic flow. Diffuse dislocation structures have been reported in such situations.[10,11,12] It should also be noted that both Eqs. [1] and [2] imply an Arrhenius temperature dependence of the strain rate with appropriate activation energies.

In this work, creep studies on an Al-2.0 wt pct Li alloy were conducted over the temperature range of 300 °C to 500 °C and the data obtained above the $\alpha + \delta$AlLi solvus were interpreted in terms of phenomenological models represented by Eqs. [1] and [2].

K.H. ELLISON, formerly with the Materials Engineering Section, Department of Mechanical Engineering, Naval Postgraduate School, is Design Engineer, Ford Motor Company, Dearborn, MI 48120. T.R. McNELLEY, Professor, and A.G. FOX, Associate Professor, are with the Materials Engineering Section, Department of Mechanical Engineering, Naval Postgraduate School, Monterey, CA 93943-5000.

Manuscript submitted January 9, 1992.

II. THEORY FOR SEQUENTIAL MECHANISMS OF DEFORMATION DURING CREEP

It has been suggested[6,7] that creep in solid solution alloys can be thought of in terms of sequential contributions to the strain made by both dislocation glide and climb. If this is so, the total strain rate, $\dot{\varepsilon}_T$, will be related to the individual contributions from climb and glide processes ($\dot{\varepsilon}_c$ and $\dot{\varepsilon}_g$, respectively) by

$$\frac{1}{\dot{\varepsilon}_T} = \frac{1}{\dot{\varepsilon}_c} + \frac{1}{\dot{\varepsilon}_g} \qquad [4]$$

In this case, the slower of the climb or glide mechanisms will dominate the total creep rate. Several factors will influence both the climb- and glide-controlled strain rates and thus the observed creep behavior. For example, in Eq. [1] (climb-controlled creep), the factor K_1 contains a stacking fault energy, γ, dependence of the form

$$K_1 = K\left(\frac{\gamma}{E\mathbf{b}}\right)^3 \qquad [5]$$

and K is a constant for many materials.[5-8] Equations [1], [4], and [5] suggest that a reduction in γ due to alloying will lead to strengthening and favor climb control of deformation.

At least two possible models have been proposed to account for deformation based on dislocation glide. When dislocation cores are saturated by solute atoms, Friedel[13] has shown that the factor A in Eq. [2] can be expressed as

$$A = \frac{2kT}{Eb} \qquad [6]$$

where k is Boltzmann's constant and T is the absolute temperature. When normal stresses and Young's modulus, E, are used, the constant K_2 will be given by

$$K_2 = \frac{\pi(1-\nu)(2(1+\nu))^2}{12} \qquad [7]$$

where ν is Poisson's ratio. Equations [2], [6], and [7] together (which do not depend on alloy composition) have been used to describe the creep behavior of Al-Mg alloys of high Mg content.[14] In this alloy system, the Mg atoms are recognized to interact strongly with dislocations, resulting in solute saturation of dislocation cores even at relatively high temperatures.[13,14] In fact, this model is able to account for the lack of Mg-concentration dependence of the creep rate in the power-law regime for alloys containing more than about 3.0 wt pct Mg.[14]

For diffuse solute distributions (unsaturated dislocation cores), the Cottrell-Jaswon[15] model can apply, and in this case,

$$A = \frac{Ee^2c\mathbf{b}^5}{kT} \qquad [8]$$

where e is the volume size difference between the solute and solvent atoms and c is the atom fraction of solute, and

$$K_2 = \frac{8\pi(1-\nu)(1+\nu)^2}{3} \qquad [9]$$

In order to determine the applicability of these two different models for glide deformation, it is necessary to know whether solute saturation of dislocation cores is expected for the creep deformation of Al-Li alloys in the temperature range of interest. Hirth and Lothe[16] have suggested that the temperature, T_0, below which solute saturation should occur, may be estimated from the equation

$$T_0 = -\frac{U_i}{k \ln c} \qquad [10]$$

where U_i is the interaction energy between solute atoms and dislocations. Based on data summarized by Friedel,[13] a plot of U_i values *vs* volume-atomic size difference for four different binary Al-based solid solutions is shown in Figure 1. Data for the volume size difference applicable to Al-Li alloys have been reported by King[17] and Fox and Fisher.[18] Their work suggests that e is 0.021 to 0.030, and so U_i lies between 0.01 and 0.04 eV/atm, as indicated in Figure 1. The corresponding range of temperatures above which solute atoms no longer saturate dislocation cores in an Al-2.0 wt pct Li alloy is thus calculated to be 45 to 179 K. This is far below temperatures at which creep is appreciable in Al-based alloys, and it is expected that Eqs. [2], [8], and [9] together would describe the glide contribution to creep deformation in Al-Li alloys.

The estimates of U_i presented in Figure 1 are based solely on the volume-atomic size difference between solvent and solute atoms. The data in this figure show good correspondence between interaction energy and volume-atomic size difference for several alloys. It has recently

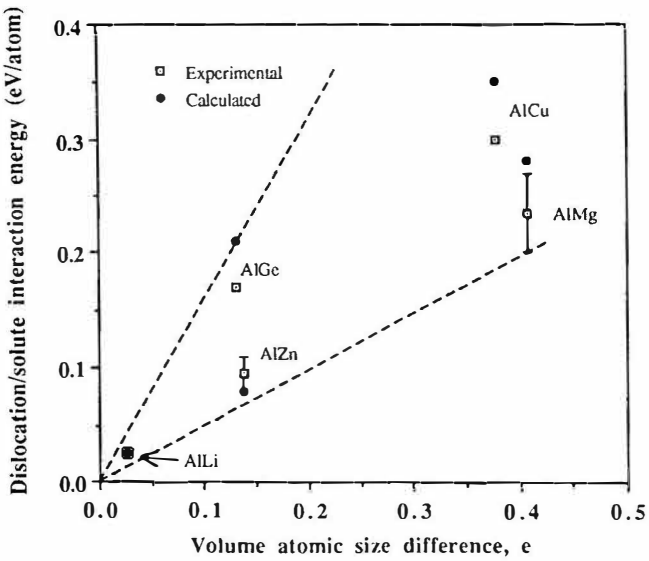

Fig. 1—Dislocation-solute interaction energy, U_i, *vs* volume-atomic size difference, e. Data (except AlLi) are taken from Friedel.[13]

been suggested[2,19] that the interaction energy U_i between solute atoms and dislocations in Al-Li alloys may be about 20 times higher than that calculated above due to the modulus difference between isolated Li atoms in solution and the surrounding matrix material. This estimate of U_i, produced by Evans,[19] is based on the rate of change of the bulk elastic properties with composition. It is implicit in this approach that the increased modulus values reflect a Li atom stiffness which is even greater than that of the Al atom replaced. Bulk Li has a much lower stiffness than pure Al, and it is difficult to see, despite electronic changes associated with alloying, how individual Li atoms in the Al-Li matrix could become substantially stiffer than individual Al atoms. Indeed, Fox and Fisher[18] have shown that the nearest neighbor (n-n) force constants associated with Li atoms in Al-Li solid solutions are significantly *lower* than the n-n force constants associated with Al atoms in these alloys. This directly contradicts the basis for Evans'[19] calculation of U_i. It should also be noted that additions (in atomic percent) of Cu and Mg change the modulus of Al at a similar rate compared to equivalent atom percent Li additions. This may be shown by analysis of the modulus data for various binary Al alloys reported by Starke.[20] Figure 1 suggests that U_i for Al-Cu and Al-Mg alloys correlates simply with the volume-atomic size difference and not with the rate of change of Young's modulus with composition. It is therefore not unreasonable to assume similar behavior for Li additions. This approach has been adopted in the present work.

The preceding suggests that the Cottrell-Jaswon approach is appropriate for modeling the glide contribution to creep in Al-Li alloys, whereas Eqs. [1], [5], and [6] can be used to describe the climb part of the total creep process. These ideas will be applied to the experimental data presented in Section III.

III. EXPERIMENTAL PROCEDURE

The alloy provided for this investigation was cast at the Naval Surface Weapons Center in White Oak, MD. High-purity (99.99 wt pct) Al and Li were melted under a controlled atmosphere. From the resulting ingot, 42-mm-thick sections were cut and homogenized by annealing at 540 °C for 12 hours. These were then hot-rolled between 400 °C and 450 °C to a final thickness of 2.0 mm. Sheet-type tensile specimens were prepared with tensile axes always parallel to the rolling direction. Just prior to testing, the machined samples were solution-treated by heating in air for 15 minutes at 500 °C followed by air cooling. Calculations based on the vapor pressure and diffusivity of Li in Al suggested minimal Li loss from sample surfaces.

Constant true-stress creep tests and constant extension-rate tensile tests were conducted at 50 °C intervals between 300 °C and 500 °C after allowing samples to equilibrate at the test temperature for 45 minutes. The applied stresses for creep testing were selected to provide creep rates between 10^{-6} and 10^{-3} s^{-1}. Nominal strain rates in the tensile tests varied from 10^{-4} to 10^{-2} s^{-1}. In addition, temperature-cycling creep tests were performed utilizing applied true stress values which gave low initial creep rates. The temperature cycling tests involved cycling in the following ranges (°C): 300 to 310, 350 to 360, 400 to 410, 450 to 460, 470 to 480, and 500 to 510. The cycle duration was sufficient in all cases to establish constant creep rates in the secondary stage of creep in order that accurate values of activation energy could be obtained.

Samples were prepared for optical microscopy by both electrolytic polishing and etching to facilitate observation using polarized light techniques. Grain contrast was achieved by use of the modified Barker's reagent (1.0 l of Barker's reagent to which 79 g of boric acid have been added). Transmission electron microscopy (TEM) was conducted on thin foils prepared with their normals parallel to the sheet normal.

IV. RESULTS

Optical microscopy (Figure 2) of solution-treated and air-cooled material just prior to testing revealed an equiaxed, coarse-grained (≈50 μm) microstructure with no evidence for the precipitation of δAlLi. The extent of strain hardening observed in the stress-strain curves decreased with increasing test temperature. As the test temperature increased, the curves exhibited an increasing regime of deformation at approximately constant stress and ductilities varied from 60 to 90 pct elongation to failure.

A typical constant true-stress creep curve is shown in Figure 3 for a test conducted at 400 °C. The curve shows features characteristic of a subgrain-forming material. In

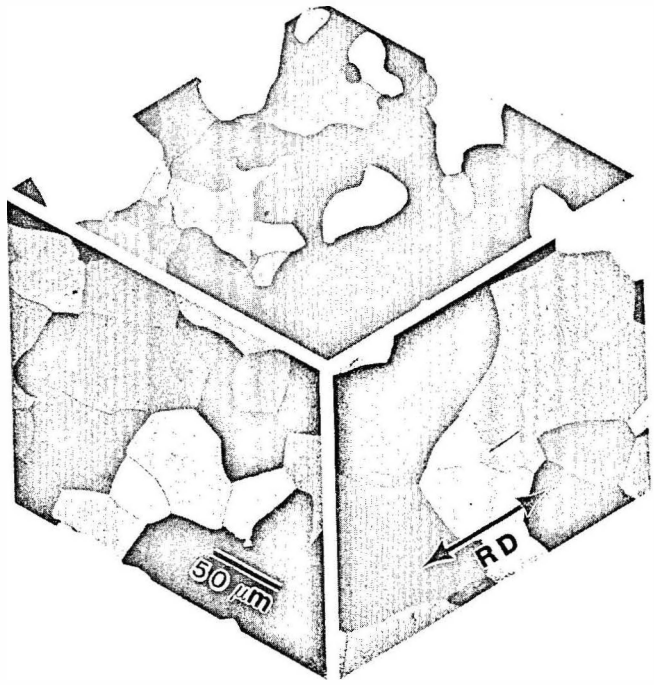

Fig. 2—Triplanar optical micrographs of the solution-treated and quenched condition prior to either creep or stress-strain testing. Samples were electrolytically etched (modified Barker's reagent) and viewed using crossed polars. The rolling direction (RD) is indicated, and the upper micrograph represents the rolling plane.

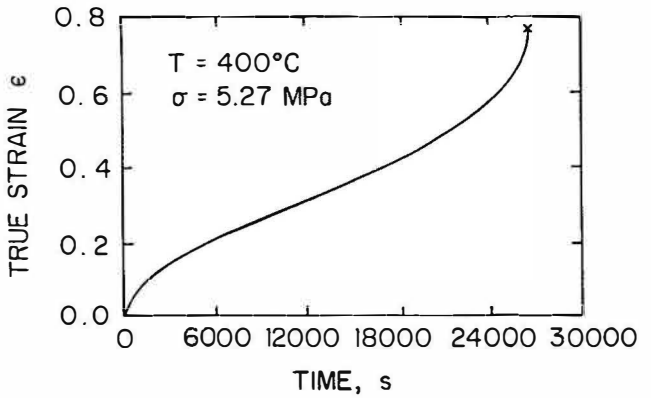

Fig. 3—A typical creep curve obtained during testing of the Al-2.0 wt pct Li alloy at 400 °C. An extensive primary stage of creep is apparent. The creep rate during secondary creep was $\dot{\varepsilon} \approx 1.71 \times 10^{-5}$ s^{-1}.

particular, a well-defined primary stage is apparent. Examination of all the test data revealed a primary stage in each case, but the extent of primary creep decreased with increasing test temperature.

The stress dependence of the deformation rate was evaluated by plotting strain rate *vs* stress on double logarithmic axes, as shown in Figure 4. These data are also summarized in Table I. The flow stress value for any particular constant extension-rate test was either the maximum or the constant stress value observed for the test in question, depending on the extent of strain hardening. The applied stress and corresponding minimum creep rate were also used to provide data for Figure 4. The stress exponent, n, was determined for each test temperature, and these results are also included on Figure 4. It is clear that n is close to five for testing conducted at 400 °C or above.

Two optical micrographs of the microstructure for a sample subjected to creep at 400 °C are shown in Figure 5. The deformed gage section (Figure 5(a)) shows evidence of subgrain formation in that the grain boundaries are serrated. These serrations most likely result from interactions between high-angle grain boundaries and the dislocation arrays which make up the subboundaries. On the other hand, Figure 5(b), which is a micrograph of the undeformed grip section, shows smooth high-angle boundaries typical of an annealed solid solution. Further evidence for subgrain formation is presented in Figure 6, which is a representative TEM micrograph of the same deformed gage section of Figure 5(a). Dislocation arrays indicative of low-angle boundaries associated with subgrains are clearly evident.

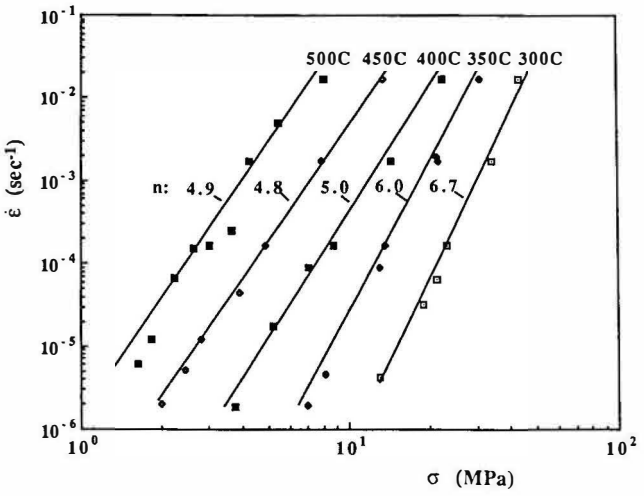

Fig. 4—The stress *vs* strain-rate data of the Al-2.0 wt pct Li obtained from both creep and constant extension rate tests. The value of the stress exponent, n, is indicated for each test temperature and is approximately 5.0 at 400 °C or above.

Apparent constant-stress activation energies, $Q_{app,\sigma}$, were determined both from the data of Figure 4 and from the temperature cycling experiments by application of the relationship

$$Q_{app,\sigma} = -R \left[\frac{\partial \ln \dot{\varepsilon}}{\partial \left(\frac{1}{T} \right)} \right]_{\sigma} \qquad [11]$$

where R is the gas constant. Within experimental error, the activation energy values obtained in this way are similar for both methods; the data are shown in Figure 7. At high temperatures, $Q_{app,\sigma}$ is about 139 *k*J/mol which is very close to the value reported by Park *et al.*[2,3] As temperature decreases in the single-phase region toward the $\alpha + \delta$ solvus (≈380 °C), $Q_{app,\sigma}$ increases to a value around 240 *k*J/mol. The data obtained at temperatures below the $\alpha + \delta$ solvus are included for completeness and indicate that $Q_{app,\sigma}$ decreases again at lower temperatures. Also included in Figure 7 are data for the temperature dependence of the observed activation energy for creep of pure Al.[5] None of these data are corrected for the temperature dependence of Young's modulus, E.

V. DISCUSSION

The observation of extensive primary creep and the presence of subgrains in samples crept into the secondary stage clearly suggest that the creep process in this Al-2.0 wt pct Li alloy is governed by dislocation climb. Further support for this assertion is provided by the measured values of the stress exponent, n, which are close to 5 for temperatures of 400 °C and above. These observations do not agree with the predictions of Park *et al.*[2,3] for creep of an Al-2.0 wt pct Li alloy in this same temperature range. Their calculations, based on the analysis of Evans[19] discussed previously, suggest that dislocation cores will be saturated by Li solutes for temperatures above the $\alpha + \delta$ solvus and that the stress exponent, n, will be equal to 3. The alloy creep behavior would then be described by Friedel's model (Eqs. [2], [6], and [7]). The present work shows that this is not the case. As discussed in Section II, the dislocation-solute interaction energy U_i, when estimated on the basis of volume atomic size difference only, indicated that dislocation cores are not saturated in this temperature range. It remains to be shown that the applicable Cottrell-Jaswon glide analysis (Eqs. [2], [8], and [9]),

Table I. Summary of Mechanical Test Results

T (°C)	$\dot{\varepsilon}$ (s^{-1})	σ (MPa)	T (°C)	$\dot{\varepsilon}$ (s^{-1})	σ (MPa)	T (°C)	$\dot{\varepsilon}$ (s^{-1})	σ (MPa)
300*	1.67×10^{-2}	43.7	350	1.93×10^{-6}	7	450	5.15×10^{-6}	2.46
300*	1.67×10^{-3}	34.4	400*	1.67×10^{-2}	22.2	450	1.99×10^{-6}	2.00
300*	1.67×10^{-4}	23.1	400*	1.67×10^{-3}	14.4	500*	1.67×10^{-2}	8.08
300	6.40×10^{-5}	21.2	400*	1.67×10^{-4}	8.71	500	4.83×10^{-3}	5.48
300	3.25×10^{-5}	19	400	9×10^{-5}	7.10	500*	1.67×10^{-3}	4.27
300	4.24×10^{-6}	13	400	1.71×10^{-5}	5.27	500	2.43×10^{-4}	3.67
350*	1.67×10^{-2}	31.1	400	1.83×10^{-6}	3.76	500*	1.67×10^{-4}	3.02
350	1.90×10^{-3}	21.2	450*	1.67×10^{-2}	13.4	500	1.50×10^{-4}	2.65
350*	1.67×10^{-3}	21.4	450*	1.67×10^{-3}	7.96	500	1.49×10^{-4}	2.65
350*	1.67×10^{-4}	13.6	450*	1.67×10^{-4}	4.90	500	6.59×10^{-5}	2.25
350	8.88×10^{-5}	12.9	450	4.43×10^{-5}	3.90	500	1.20×10^{-5}	1.84
350	4.47×10^{-6}	8.08	450	1.22×10^{-5}	2.80	500	6.00×10^{-6}	1.63

*Denotes constant extension rate test.

Table II. Creep Activation Energy Measurements by Temperature Cycling

T_{lo}–T_{hi} (°C)	Mean T (°C)	σ (MPa)	$\dot{\varepsilon}_{lo}$ (s^{-1})	$\dot{\varepsilon}_{hi}$ (s^{-1})	$Q_{app,\sigma}$ (kJ/mol)
300 to 310	305	11.9	2.10×10^{-6}	4.30×10^{-6}	198.5
350 to 360	355	6.80	1.28×10^{-6}	6.55×10^{-6}	219.0
400 to 410	405	3.03	1.18×10^{-6}	2.22×10^{-6}	240.7
400 to 410	405	3.03	3.98×10^{-7}	7.31×10^{-7}	231.5
450 to 460	455	2.46	5.51×10^{-6}	8.69×10^{-6}	229.9
470 to 480	475	2.03	1.75×10^{-6}	2.52×10^{-6}	169.1
500 to 510	505	1.64	1.51×10^{-6}	1.99×10^{-6}	138.6

combined with the climb model (Eq. [1]), is a satisfactory description of the experimental results presented here.

The present results suggest that $\dot{\varepsilon}_g$, the glide creep rate in Eq. [4] is so large that the time spent in glide is very small compared with that spent in climb and thus the climb creep rate, $\dot{\varepsilon}_c$, dominates in Eq. [4]. This conclusion can be verified by directly calculating $\dot{\varepsilon}_g$ and comparing the results to corresponding values of $\dot{\varepsilon}_c$ for pure Al. It is not possible to calculate $\dot{\varepsilon}_c$ for the Al-Li alloy in question, because the effect of Li on the stacking fault energy, γ, is unknown. However, $\dot{\varepsilon}_c$ for the alloy is expected to be lower than the corresponding rate for pure Al as Li additions significantly increase the modulus and alloying generally lowers the stacking fault energy in face-centered cubic metals (Eqs. [1] and [4]).

Calculations of $\dot{\varepsilon}_g$ for T = 673 to 773 K (400 °C to 500 °C) based on Eqs. [2], [8], and [9] (the Cottrell-Jaswon approach) were made with $\nu = 0.3$, $e = 0.021$, $c = 0.074$ (2.0 wt pct), and $\mathbf{b} = 2.8 \times 10^{-10}$ m. Data for the temperature-dependent Young's modulus of pure Al were employed.[21] This calculation also requires values for D_{sol}. Data reported by Williams and Edington[22] provide upper and lower bounds for D_{Li} in units of m^2/s. These are $8.3 \times 10^{-4} \exp(-15.9/T) > D_{Li} > 2.4 \times 10^{-3} \exp(-17.8/T)$, where T is the absolute temperature (K). Using these bounds, the predicted strain-rate *vs* stress responses for the Cottrell-Jaswon model at T = 673 K (E_{673K} = 54.9 *GPa*) are compared in Figure 8 to the experimental results for this temperature. It is clear from this figure that the glide-based model predicts much higher strain rates than observed experimentally, and this is consistent with climb as the rate-controlling process. Also shown in Figure 8 is a line corresponding to Eq. [1] for climb-controlled creep in pure Al at this temperature.[9] The Al-Li alloy is stronger than pure Al, and this is likely the result of modulus and stacking fault energy effects due to the Li addition.

For pure metals and alloys which follow Eq. [1], the observed creep activation energies are nearly equal to activation energies reported for self-diffusion or perhaps dislocation core diffusion.[23,24] It has been demonstrated for pure Al that the temperature dependence of Young's modulus, E, can account for small differences between creep activation energies at high temperatures and the activation energy for lattice diffusion.[5] The activation energy for lattice diffusion, Q_l, for pure Al is about 142.3 kJ/mol.[23] For Al-Li alloys, the activation energy for Li diffusion is between 131.9 and 146.5 kJ/mol which is very similar.

In the present work, the observed activation energy for creep, $Q_{app,\sigma}$, in the range 475 °C to 500 °C was found to agree closely with the activation energy value reported by Park *et al.*[2,3] at 525 °C, as shown in Figure 7. In turn, both of these values are close to the activation energies for diffusion of Al or Li in Al-Li alloys.[22,23] As the temperature is decreased in the range of the single-phase solid solution, $Q_{app,\sigma}$ increases from around 139 kJ/mol at 500 °C to about 240 kJ/mol at 400 °C and then appears to decrease upon passing below the $\alpha + \delta$ solvus. This anomalous temperature dependence of the activation energy for creep suggests that the factors governing creep in the alloy are more strongly temperature dependent than in pure Al. A possible explanation for this can be developed from Eqs. [1] and [5]. If it is assumed that

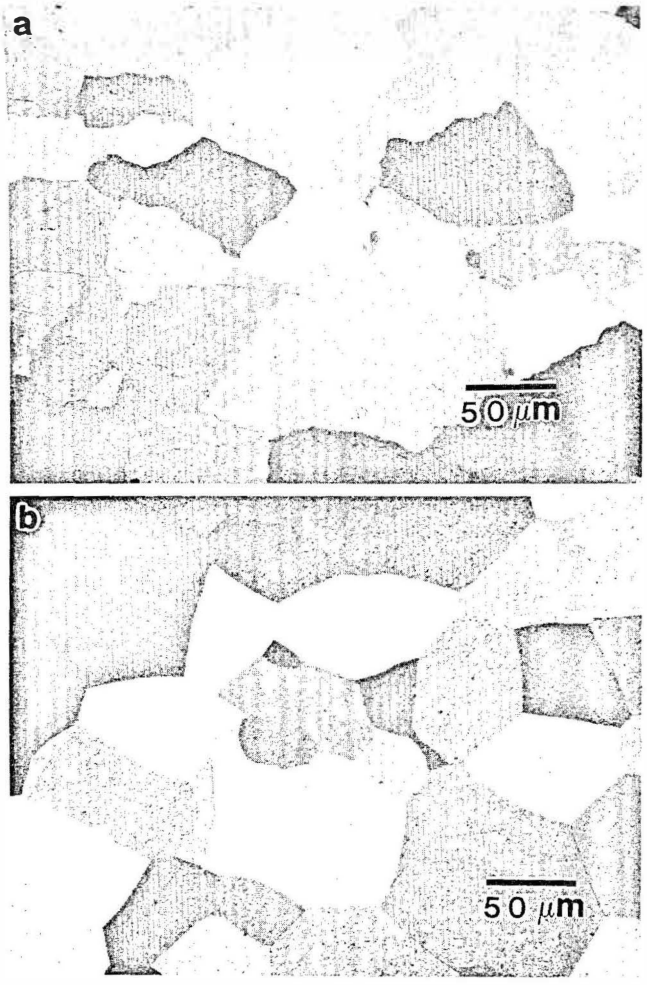

Fig. 5—Optical micrographs taken using crossed polars from (*a*) the deformed gage section and (*b*) the undeformed grip section of a sample crept into steady state at T = 400 °C and σ = 10.2 MPa and then cooled under load. The creep rate at test termination was ≈ 5.5 × 10^{-4} s^{-1}. Samples were electrolytically etched using the modified Barker's reagent.

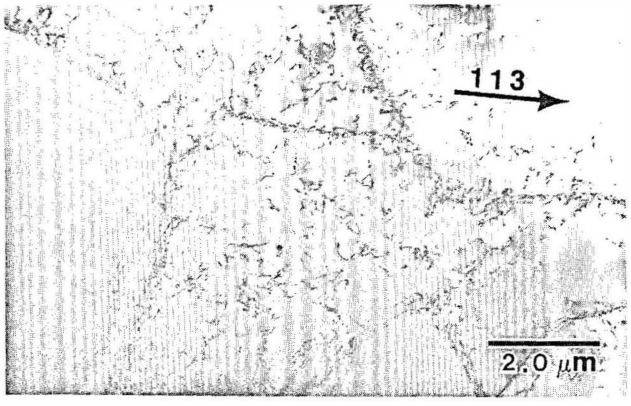

Fig. 6—A bright-field transmission electron micrograph of the deformed gage section from the sample of Figure 5 illustrating subgrain formation during creep of this alloy. The sample was crept into steady state at T = 400 °C and σ = 10.2 MPa and then cooled under load.

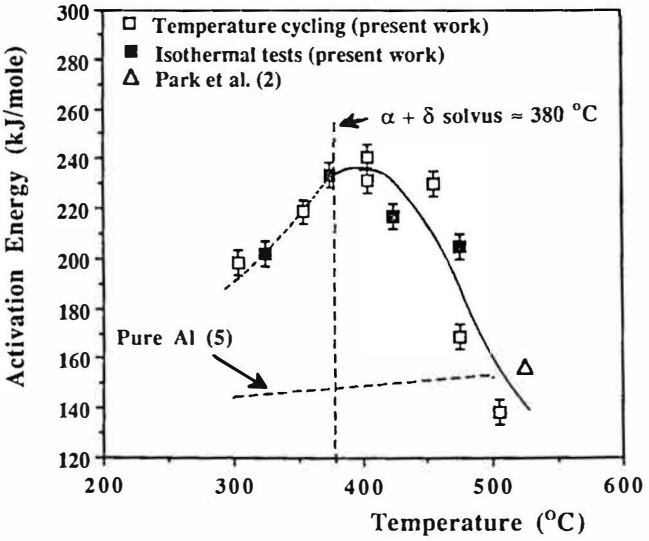

Fig. 7—Apparent activation energy *vs* temperature from both the stress *vs* strain-rate data of Figure 4 and the temperature cycling data of Table II. The $Q_{app.,\sigma}$ values are plotted *vs* the corresponding average of the test temperatures involved in the calculation.

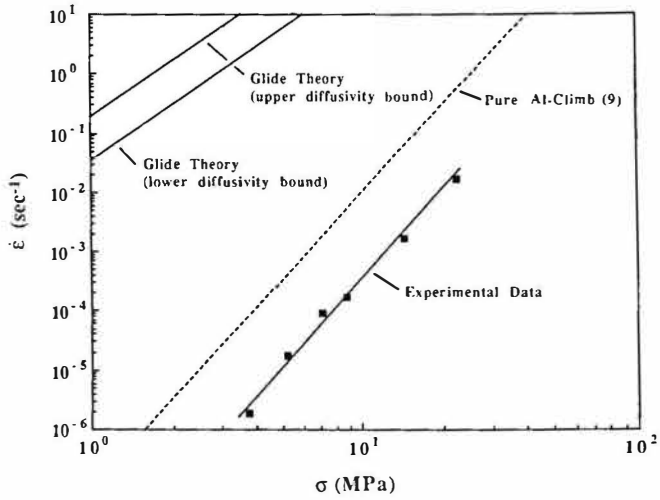

Fig. 8—A comparison between the experimental strain-rate *vs* stress data obtained at T = 400 °C in this research and the predicted strain-rate *vs* stress response according to the glide-controlled model using the Cottrell-Jaswon analysis. The glide-controlled model predicts a creep rate several orders of magnitude greater than that observed, and this is consistent with climb control of creep in this alloy. Also shown for comparison are data for creep of pure Al which is climb controlled in this regime.[9]

these equations describe creep in the alloy, then the activation energy at constant stress, Q_σ, may be derived as[5]

$$\frac{Q_a}{R} = -\left.\frac{\partial \ln \dot{\varepsilon}_c}{\partial\left(\frac{1}{T}\right)}\right|_\sigma = -3\frac{\partial \ln \gamma}{\partial\left(\frac{1}{T}\right)} + 8\frac{\partial \ln E}{\partial\left(\frac{1}{T}\right)} + \frac{Q_D}{R} \quad [12]$$

where Q_D is the activation energy for diffusion and the Burgers vector, **b**, is assumed to be constant. Equation [12] indicates that if the stacking fault energy

and elastic modulus are independent of temperature, then $Q_{app,\sigma} = Q_\sigma = Q_D$ at all temperatures. As noted earlier, small but significant differences between $Q_{app,\sigma}$ and Q_D in pure Al have been shown to result from the modulus term in Eq. [12].[5]

It is possible that the anomalous temperature dependence of creep in this Al-2.0 wt pct Li alloy could arise from a more pronounced change with temperature in either the stacking fault energy or the modulus. Indeed, Sigli and Sanchez[25] and Khachaturyan *et al.*[26] have predicted that a disorder-order transformation can occur upon cooling of alloys similar in Li content to that of the present work at temperatures in the range of those studied here. Interatom bond strengths in an initially disordered fcc solid solution will almost certainly change upon ordering and the formation of domains of the ordered $L1_2$ structure. This, in turn, will contribute to the temperature dependence of the stacking fault energy and elastic modulus as the extent of ordering varies with temperature. Effects associated with the transition, which has been shown to occur experimentally,[27,28,29] could be responsible for such changes, although the range of temperatures over which ordering occurs has not yet been measured. In addition, independent measurements of the temperature dependence of the stacking fault energy and elastic modulus would be required to resolve this question.

ACKNOWLEDGMENTS

The authors would like to thank Dr. A.P. Divecha, Naval Surface Weapons Center, White Oak, MD, for providing the alloy used in this work. Thanks are also due to Professor D.K. Matlock, Colorado School of Mines, Golden, CO, and Dr. D. Michel of the Naval Research Laboratory, Washington, DC, for useful discussion of this work. This article was prepared for the Naval Air Systems Command (Dr. L.E. Sloter as monitor) with funding from the Naval Postgraduate School.

REFERENCES

1. E.A. Starke, T.H. Sanders, and I.G. Palmer: *J. Met.*, 1981, vol. 33 (8), pp. 24-33.
2. K.-T. Park, E.J. Lavernia, and F.A. Mohamed: *Acta Metall. Mater.*, 1990, vol. 38, pp. 1837-48.
3. K.-T. Park, E.J. Lavernia, and F.A. Mohamed: in *Aluminum-Lithium Alloys (vol. II), Proc 5th Int. Aluminum-Lithium Conf.*, T.H. Sanders and E.A. Starke, eds., Materials and Component Engineering Publications Ltd., Birmingham, United Kingdom, 1989, pp. 1155-62.
4. A.J. McAlister: *Bull. Alloy Phase Diagrams*, 1982, vol. 3, pp. 177-83.
5. O.D. Sherby and P.M. Burke: *Prog. Mater. Sci.*, 1968, vol. 13, pp. 325-90.
6. W.R. Cannon and O.D. Sherby: *Metall. Trans.*, 1970, vol. 1, pp. 1030-32.
7. F.A. Mohamed and T.G. Langdon: *Acta Metall.*, 1974, vol. 22, pp. 779-88.
8. A.K. Mukherjee, J.E. Bird, and J.E. Dorn: *Trans. ASM*, 1969, vol. 62, pp. 155-79.
9. M.Y. Wu and O.D. Sherby: *Acta Metall.*, 1984, vol. 32, pp. 1561-72.
10. J. Weertman: *J. Appl. Phys.*, 1957, vol. 28, pp. 1185-89.
11. S. Takeuchi and A.S. Argon: *J. Mater. Sci.*, 1976, pp. 1542-54.
12. W.C. Oliver and W.D. Nix: *Acta Metall.*, 1982, vol. 30, pp. 1335-47.
13. J. Friedel: *Dislocations*, Addison-Wesley, Reading, MA, 1964, pp. 356-410.
14. T.R. McNelley, D.J. Michel, and A. Salama: *Scripta Metall.*, 1989, vol. 23, pp. 1657-62.
15. A.H. Cottrell and M.A. Jaswon: *Proc. R. Soc., London*, 1949, vol. A199, pp. 104-114.
16. J.P. Hirth and J. Lothe: *Theory of Dislocations*, McGraw-Hill, New York, NY, 1968, p. 468.
17. H.W. King: *J. Mater. Sci.*, 1966, vol. 1, pp. 79-90.
18. A.G. Fox and R.M. Fisher: *Acta Cryst.*, 1987, vol. A43, pp. 260-65.
19. J.T. Evans: *Scripta Metall.*, 1987, vol. 21, pp. 1435-38.
20. E.A. Starke: in *Proc. 6th Intl. Conf. on the Strength of Metals and Alloys*, R. C. Gifkins, ed., Pergamon Press, Oxford, United Kingdom, 1982, pp. 1025-31.
21. W. Köster: *Z. Metallkd.*, 1948, vol. 39, pp. 1-9.
22. D.B. Williams and J.W. Edington: *Phil. Mag.*, 1974, ser. 8, vol. 30, pp. 1147-53.
23. T.S. Lundy and J.F. Murdock: *J. Appl. Phys.*, 1962, vol. 33, pp. 1671-79.
24. J. Askill: *Tracer Diffusion Data for Metals, Alloys and Simple Oxides*, IFI/Plenum, New York, NY, 1970, p. 11.
25. C. Sigli and J.M. Sanchez: *Acta Metall.*, 1986, vol. 34, pp. 1021-28.
26. A.G. Khachaturyan, T.F. Lindsey, and J.W. Morris, Jr.: *Metall. Trans. A*, 1988, vol. 19A, pp. 249-57.
27. V. Radmilovic, A.G. Fox, and G. Thomas: *Acta Metall.*, 1989, vol. 37, pp. 2385-94.
28. A.G. Fox, S.C. Fuller, C.E. Whitman, and V. Radmilovic: *J. Mater. Res.*, 1991, vol. 6, pp. 712-18.
29. G. Schmitz and P. Haasen: *Acta Metall. Mater.*, 1992, vol. 40, pp. 2209-17.